Biocatalysis and Agricultural Biotechnology 22 (2019) 101434

Contents lists available at ScienceDirect

Biocatalysis and Agricultural Biotechnology

journal homepage: http://www.elsevier.com/locate/bab

Efficient removal of a glyphosate-based herbicide from water using ZnO nanoparticles (ZnO-NPs)

Mauricio Rodríguez Páez [a], Y. Ochoa-Muñoz [b], J.E. Rodriguez-Páez [b, *]

[a] Masters Student in Environmental Sciences, Jorge Tadeo Lozano University, Bogotá, Colombia
[b] CYTEMAC Group – Department of Physics/FACNED, University of Cauca, Popayán, Colombia

ARTICLE INFO

Keywords:
ZnO-NPs
Synthesis
Characterization
Glyphosate removal
Adsorption

ABSTRACT

Though there may not be consensus regarding the toxicity of glyphosate, given the strong interest in its removal from water sources nanotechnology was used in this work to that end. Nanoparticles of zinc oxide (ZnO-NPs) were synthesized in a controlled manner by chemical route. The ZnO powders were then characterized by infrared and UV–Vis absorption spectroscopies, X-ray diffraction and scanning electron microscopy. To evaluate the capacity for removal, aqueous solutions of the Monsanto herbicide Roundup 747 SG containing 679 g/kg of glyphosate were adjusted to obtain glyphosate-ZnO-NP suspensions of 250 ppm–250 ppm, 700 ppm–700 ppm, 1000 ppm–1000 ppm, 1000 ppm–250 ppm and 1000 ppm–700 ppm and these were used to carry out the tests. The % Removal curves obtained indicate that the ZnO-NPs removed between ~70% and 90% of the herbicide in the system. While the UV–Vis absorption spectra showed small displacements of the absorption maximum and the appearance of other small bands, indicating herbicide degradation, adsorption proved to be the most important removal mechanism. The kinetics of the process was suitably described by a pseudo second order equation, although it is not possible to rule out, for some glyphosate-ZnO-NP concentration ratios, the importance of intraparticle diffusion. These results indicate that the synthesized ZnO nanoparticles were efficient in the removal of glyphosate in aqueous solutions at the laboratory level.

1. Introduction

The need to address the problem of food scarcity began to become evident in the mid-twentieth century. The increase in world population has encouraged technological developments to increase food production - mainly agricultural production with sustainable agriculture in mind (P. Tittonell, 2014; Pretty et al., 2003). With the advances in the field of agriculture, crop management techniques have been developed and adopted by farmers around the world. This has encouraged the use of large amounts of pesticides, including herbicides, to protect plants against pests, fungi and weeds. When a human being ingests pesticides, by accident or through daily exposure, these can cause various diseases in the skin, eyes and nervous system; if exposure is very prolonged, it can cause cancer (Rawtani et al., 2018).

The residue of these agrochemicals can become widely dispersed in drinking waters, groundwaters and soils (Taghizade et al., 2018; Nasrabadi et al., 2011; Grillion et al., 1999). Prominent among the routes that would lead to contamination of the environment with pesticides are land runoff, direct entry from product spraying, industrial effluents and dust. Taking into account the usual process of spraying pesticides on crops, more than 90% of the dispersed product reaches destinations other than those targeted. This causes the agrochemicals to persist in the soil and reach water bodies (Damalas and Elefthero Horinos, 2011). Pesticide residues significantly affect aquatic ecosystems and mammals. Considering specifically the quality of water for human consumption, the presence of pesticides significantly lowers water quality (Khatri et al., 2016). The Drinking Water Directive (98/83/EC) defines a limit of 0.1 μg/L for any single pesticide and 0.5 μg/L for the sum of all pesticides detected and measured through normal monitoring (Plakas and Karabelas, 2012). Thus, there is an urgent need to detect pesticides and remove them from sources of drinking water. With this in mind, innovative methods have been developed with the aim of efficiently treating water. Those rooted in nanotechnology stand out, due to the fact that a number of nanomaterials boast physicochemical properties that position them as good candi-

* Corresponding author. Universidad del Cauca. Calle 5 N° 4-70, Popayán – Cauca, Colombia.
E-mail address: jnpaez@unicauca.edu.co (J.E. Rodriguez-Páez).

https://doi.org/10.1016/j.bcab.2019.101434
Received 25 July 2019; Received in revised form 11 November 2019; Accepted 15 November 2019
Available online 18 November 2019
1878-8181/Published by Elsevier Ltd.

dates for removing pesticides from water beds (Rawtani et al., 2018; Taghizade Firozjaee et al., 2018).

In addition, with the development of new technologies, the limits of these pesticides extend to health risks that reach right to the molecular level, in other words that just a few molecules of these agrochemicals can cause adverse effects on the health of the population. That is why a technology is required that works at atomic and molecular levels, both to detect and to degrade pesticides (Rawtani et al., 2018). As regards proposed methodologies based in nanotechnology, evaluations have been carried out for adsorption (Moradi Dehaghi et al., 2014; Tovakkoli and Yazdanbakhsh. 2013), nanofiltration (Plakas and Karabelas, 2012; Van der Bruggen et al., 1998) and degradation (Abdennouri et al., 2016; Navarro et al., 2009; Keum and Li, 2004).

More specífically, Glyphosate, N-(Phosphonomethyl)glycine (GLY) is a herbicide with a non-selective, broad-spectrum activity. It was introduced in 1974 for the control of agricultural production areas (Benbrook, 2016) and is one of the most widely used herbicides worldwide (Woodbruen, 2000; Castle et al., 2004), a situation favored by the introduction of genetically modified GLY-resistant crops at the end of the 20th century. Glyphosate is not normally applied in its pure form, but in commercial formulations such as Roundup (Monsanto, 2002, 2013) and Touchdown (Syngenta), which are called glyphosate-based herbicides (GBHs). The similarities with Phosphoenolpyruvate (PEP) allow glyphosate to bind to the 5-enolpyruvylshikimate 3-phosphate (EPSP) synthase substrate to inhibit its activity and block its integration in the chloroplast. The inhibition of the functioning of the shikimate pathway generates a deficiency in aromatic amino acids, which eventually causes the death of the plant due to malnutrition. In addition to glyphosate, GBHs contain several adjuvants (Li et al., 2005), among them those that increase the adhesion of glyphosate to the surface of plants (for example alkylpolyglycoside), which facilitate penetration into the cell walls of plants and their tissues (e.g. ethoxylated tallow amines) to exert their herbicidal effects. Unfortunately the full composition of GBHs is not known. This is treated as a trade secret by manufactures, and available data on the hazards posed by different mixtures remains limited (LVanderberg et al., 2017). A small number of controlled studies carried out in laboratories, using contemporary scientific approaches, have registered adverse effects, both of glyphosate and of GBHs, in doses much lower than those used to make risk assessment decisions. Specifically, Roundup contains, in addition to glyphosate, isopropylamine and polyoxyethylene amine (POEA), to improve the absorption and translocation of the active ingredient by the plants (Tsui and Chu, 2003). GBHs are used in many agricultural activities, such as control of weeds that affect crops, due to its wide range of action and the functionality for which the product was designed. In addition, other glyphosate uses have been determined, being able to be used in the chemical maturation of seeds and in sugarcane.

Research carried out by Goldsborough and Beck (1989) concluded that glyphosate is rapidly dissipated from the surface waters of lentic systems. It is further suggested that the main forms of glyphosate loss in the water column are due to adsorption by the sediment and biodegradation (Rueppel et al., 1977; Monsanto, 2014). Mann and Bidwell (1999) determined that glyphosate isopropylamine is practically non-toxic as there is no mortality among the tadpoles of any of the four species of Australian frogs studied and they mention the importance of evaluating the persistence of the surfactant components in commercial formulations of glyphosate because this factor is the main contributor of its acute toxicity; the polyoxyethyleneamine surfactant in the case of Roundup. The negative effects on the environment, for example on the amphibian population due to the contamination of water sources (Bernal et al., 2009a; Bernal et al., 2009b) cannot therefore simply be ignored. Meanwhile, because glyphosate can be degraded by soil microbes (Zhang et al., 2015) and can be linked to soil colloids (González-Martínez et al., 2005), the World Health Organization et al. (1994) considered that GLY is “toxicologically harmless” for humans, other mammals, birds and the environment (Tsui and Chu, 2003). Nevertheless, recent research suggest that GLY may be considered toxicologically harmful and presents potential association with human carcinogenesis and other chronic diseases (Valle et al., 2019; Tarazona et al., 2017) including alterations in the mental and reproductive behavior of humans (Anifandis et al., 2018; Williams et al., 2012). In a recent review (Van Bruggen et al., 2018), reference was made to the fact that, in spite of the fact that glyphosate has been used extensively in the last 40 years, opinion as to the potential risk, direct and indirect, of the use of this herbicide on human and environmental health has recently seen an increase (Conrad et al., 2017). Additionally, the scientific literature indicates that chronic exposure to GLY can lead to such diseases in humans as attention deficit hyperactivity disorder (ADHD), diabetes, heart disease, colitis, multiple sclerosis, depression, non-Hodgkin lymphoma and Alzheimer's disease (Samsel and Seneff, 2013), autism (Beecham and Seneff, 2015), chronic kidney disease (Jayasumana et al., 2014), Parkinson's disease (Gui et al., 2012), problems in pregnancy (Benachour and Séralini, 2009), among others (see Valle et al., 2019). Recent work indicates that additional work is required in higher organisms using the pesticide formulations to learn more about the potential risk of neurodegeneration in humans (Burchfield et al., 2019).

The study conducted by Romano et al. (2010), found that glyphosate significantly changes the pubertal development of male Wistar rats in a dose-dependent manner; reducing the production of testosterone and significantly decreasing the epithelial thickness of the seminiferous ducts, suggesting that the commercial glyphosate formulation is a potent endocrine disruptor *in vivo* in the reproductive development in rats when exposure is during the period of puberty (Dai et al., 2016); this agrees with the conclusions of Dallegrave et al. (2007) that the commercial formulation of glyphosate (Roundup) induces adverse reproductive effects in male Wistar rats during prenatal and postnatal exposure; a decrease in the number of sperm during the adult stage, an increase in the percentage of abnormal sperm and a decrease in the serum level of testosterone at puberty, in bullfrogs. According to Rissol et al. (2016), all the herbicides cause marked alterations in the skin, modification in the morphology of the cell wall, while the epithelial tissue can present hyperplasia or hypertrophy.

According to the literature published in recent years, it has been shown that the handling of glyphosate, as well as of the great majority of pesticides, by the rural population is unsafe (Campuzano-Cortina et al., 2017). Studies have shown the presence of this herbicide in the body of people who are exposed through work or involuntarily (Conrad et al., 2017), even in children due to inadequate storage conditions, and this is due to the fact that this toxic substance has not only gastrointestinal, but also mucocutaneous and inhalatory absorption. A particular situation occurs in countries like Colombia where glyphosate is used in the forced eradication of coca crops (Reyes, 2014), specifically by aerial spraying (Camacho and Mejía, 2017), which has caused health problems in the fields where spraying was carried out (Solomon et al., 2009).

For the degradation of glyphosate, microbial transformation is perhaps the main route, passing through fleeting intermediaries such as AMPA, sarcosine and formaldehyde, to carbon dioxide. In the case of abiotic degradation, the amounts of glyphosate degraded by non-microbial forms of decomposition are negligible; photodegradation by sunlight of glyphosate applied to the soil appears to be negligible, according to a study by PTRL, Inc., 1989 (Ahrens, 1994). Meanwhile, if biodegradation with bacterial strains is considered, various types of bacteria are used as indicated by Méndez-Villaquirán in his work (Méndez-Villaquirán, 2015), finding a certain capacity to decompose and degrade glyphosate. In most laboratory experiments, the rate of degradation of glyphosate in soils appears to be relatively rapid (Wang T. et al., 2016b, Bott et al., 2011).

Other chemical and physicochemical methods are used to degrade glyphosate (Assalin et al., 2010), noteworthy among them advanced oxidation processes (Kudzin et al., 2019), specifically the use of a TiO_2 photocatalyst (Shifu et al., 2007), hydrogen peroxide irradiated with UV (Manassero et al., 2010), TiO_2 particles doped with Mn, Ce or La and activated with visible light (Umar et al., 2016), titania nanotubes doped with photocatalytically activated cerium (Xue et al., 2011), photodegradation using goetite and magnetite (Yang et al., 2018), a nanocomposite of $BiOBr/Fe_3O_4$ (Cao et al., 2019), MnO_2 (Jaisi et al., 2016) and $BiVO_4$ (Huo et al., 2017). In addition, adsorption on a $MnFe_2O_4$-graphene hybrid compound (Yamaguchi et al., 2016), oxidative degradation with manganese oxide (Barret and McBride, 2005) and oxidation of electrochemically assisted MnO2 (Lan et al., 2013), have all been used, among other methods. Moreover, nanotechnology recently began to be used in order to degrade glyphosate. Although the number of studies carried out considering this functionality of nanoparticles is in the early stages, there are studies such as (Wang M., 2016a), who use nanoparticles of MnO_2/C, with high specific surface and high dispersion, obtaining a very strong catalytic adsorption and degradation of glyphosate. An efficient glyphosate removal was further achieved using nanosized copper hydroxide modified resin (D201Cu) (Zhou et al., 2017).

In the present work a synthesis method was structured that made it possible to obtain, in a controlled and reproducible way, ZnO nanoparticles (ZnO-NPs) which were characterized and then used to remove glyphosate from aqueous solutions previously designed in the laboratory. These nanoparticles showed a good efficiency in the removal of the herbicide.

2. Materials and methods

2.1. Synthesis of ZnO nanoparticles

The method used for the synthesis of the ZnO-NPs was that of controlled precipitation (Rodríguez-Páez, 2001; Rodríguez-Páez et al., 1997). The process was conducted at room temperature (22 °C) using distilled water (400 mL) as solvent, hydrated zinc acetate ($Zn(CH_3COO)_2$ - Merck) as Zn precursor to acidify the nitric acid system (HNO_3 - Merck) and ammonium hydroxide (NH_4OH-Merck) as precipitant. With the solvent under continuous stirring, the precursor was added and the system was allowed to acquire a transparent condition, the solution reaching a pH value of 6.4 ± 0.1.

The ammonium hydroxide (precipitating agent) was then added to the solution, an action that was carried out slowly and periodically, every 5 s, administering an amount of approximately 0.110 mg (two drops). The controlled and periodic addition of NH_4OH was carried out so that the chemical reactions, mainly of hydrolysis (favoring the presence of OH groups in the Zn^{2+} coordination sphere), could develop favorably. Each molecule of ammonium hydroxide was dissociated releasing hydroxyl, which increased the pH of the suspension, promoting the deprotonation of the water molecules that surrounded the Zn^{2+} and thus favoring the presence of hydroxy OH groups in the coordination sphere of the cation. The precipitating agent continued to be added to the system until reaching the final working pH (8.5). With the addition of NH_4OH to the system, up to pH 8.5, the hydrolysis and condensation reactions of the Zn species were favored and the development of the most important stages of the process was facilitated: embrionation, nucleation and formation of the solid precipitate (Rodríguez-Páez, 2001).

2.2. Characterization of the synthesized ZnO-NPs

To determine the physicochemical characteristics of the synthesized ceramic powders, a number of characterization techniques were used.

2.2.1. X-ray diffraction - XRD

The XRD technique allows the determination of the crystalline structure of solid samples, which defines their physical properties, including electrical, optical and catalytic properties. In this work, the diffractograms of the samples of interest were taken using the PANalytical X'Pert Pro X-ray equipment with a copper anode, Cu $k_\alpha = 1.540598 \mathring{A}$, in the range between 20° and 70°. The Scherrer formula ($D = \frac{k\lambda}{B \cos \theta}$) was used to determine the crystallite size.

2.2.2. Scanning electronic microscopy (SEM)

To observe the solids of interest for this investigation, the Tescan Vega 3 SB microscope was used. This equipment operates with a tungsten filament at accelerating voltages between 200V and 30 kV, with gaps from 0.009 Pa to 2000 Pa (pascal) and has three detectors: secondary electrons (SE), backscattered electrons (BSE) for image observation and dispersive energy X-ray spectroscopy (EDX) for elemental analysis.

2.2.3. Infrared spectroscopy

The IR spectra give information about the functional groups present in the samples. The equipment used for this test was the Thermo Scientific Nicolet iS10 FT-IR spectrophotometer. The sample was prepared using the solid of interest with KBr, to form a pellet, and the IR spectrum was recorded in the region between 4000 and 400 cm^{-1} with a resolution of 4 wave numbers.

2.2.4. UV–Vis absorption spectroscopy

Ultraviolet–visible spectrometry or UV–Vis spectrophotometry involves photon spectroscopy in the ultraviolet–visible radiation region. This technique principally considers the electronic transitions from the basal state to the excited state. For the present study, the Thermo Scientific Evolution 300 UV-VIS spectrophotometer was used.

2.3. Evaluation of glyphosate removal by ZnO-NPs

Having obtained the ZnO-NPs, using the method of controlled precipitation described above, we proceeded to quantitatively study their use in the removal of glyphosate. Initially the calibration curve of the water-glyphosate system was obtained. For this, the UV–Vis spectra of aliquots of glyphosate solutions containing concentrations from 250 to 5000 ppm of the herbicide were taken. The solutions were formed by dissolving an adequate amount of Monsanto Roundup 747 SG, which contained a glyphosate a. i. concentration of 679 g/kg, in a suitable volume of water to form the solutions in the concentrations indicated previously. For each aliquot of interest, the UV–Vis spectrum was taken and the maximum absorbance value of the glyphosate characteristic band, located at 193 nm, was recorded for the different concentrations. These data were used to correlate the values of absorbance, corresponding to the characteristic band of glyphosate, with those of the concentration of this compound in solution, obtaining the equation of the calibration curve of the system.

To determine the catalytic activity of the synthesized ZnO-NPs, evaluating the removal of glyphosate, suitable amounts of Roundup 747 SG product were weighed and dissolved in an adequate volume of water to obtain concentrations of 250, 700 and 1000 ppm. The spectra corresponding to these suspensions had been previously recorded and showed absorbance values lower than 1.5, absorbance values adequate for carrying out the study, in contrast to the values recorded for concentrations greater than 1000 ppm that were greater than 1.7. In order to evaluate the glyphosate removal capacity of the synthesized ZnO, quantities of this oxide were added to the glyphosate solutions to obtain concentrations of 250, 700 or 1000 ppm of ZnO. Subsequently, the behavior of the water-glyphosate-ZnO systems was monitored by taking aliquots of the system every 10 min for 1 h and the corresponding UV–Vis absorption spectrum was recorded, paying at-

tention to the absorbance value of the peak of maximum absorbance (located at 193 nm). Table 1 shows the glyphosate-ZnO concentration ratios evaluated through the methodology indicated above.

The previously obtained calibration curve was used to determine, based on the values of maximum absorbance (peak at 193 nm), the concentration of glyphosate present in the solution for each aliquot taken regularly over time (every 10 min). Using the values obtained, the C/C_o and % Removal ($(C_o–C)/C_o$) curves were plotted, as a function of time, to determine the capacity of glyphosate removal by the ZnO-NPs.

Table 1

Glyphosate-ZnO concentration ratios used to study the glyphosate removal capacity of the synthesized ZnO-NPs.

Roundup (ppm)	ZnO (ppm)		
	250	700	1000
250	✓	✓	✓
700		✓	✓
1000			✓

3. Results and discussion

3.1. Synthesis process

The description of the process of controlled precipitation was carried out using the potentiometric titration curve of the $Zn(CH_3COO)_2 – H_2O–HNO_3$ system (Fig. 1(a)) and that can also be used as a means of controlling the process, to ensure its reproducibility and therefore the characteristics of the final product. In it, the stages of the process are clearly differentiated because the hydrolysis and condensation reactions, which involve protons (H^+) and hydroxyl groups (OH^-), predominate (see Rodríguez-Páez et al., 2001).

3.2. Characterization of the synthesized ZnO-NPs

3.2.1. XRD

The peaks of the diffractogram in Fig. 1(b) correspond to ZnO (PDF-2 2004 according to the International Center for Diffraction Data - PDF 2004), which has a wurtzite-like crystal structure. The slenderness of the peaks indicates that the sample is well crystallized.

A further piece of information that can be obtained from the X-ray diffraction data is the crystallite size of the synthesized ZnO and for this the Debye-Scherrer formula was used:

$$d = \frac{K\lambda}{\beta \cos(\theta)} \quad (3)$$

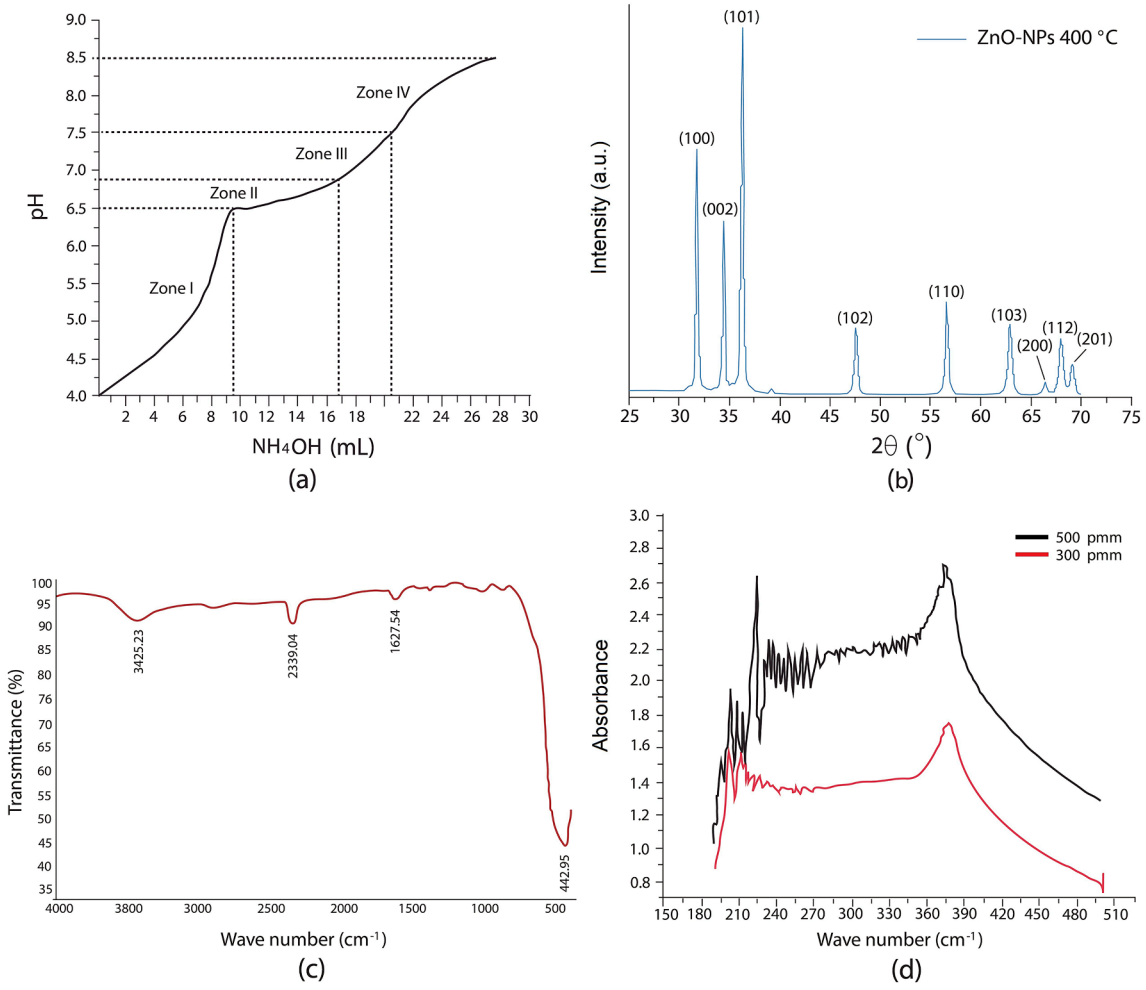

Fig. 1. (a) Potentiometric titration curve of the $Zn(CH_3COO)_2 – H_2O–HNO_3$ system and (b) X-ray diffractogram, (c) IR spectrum and (d) UV–Vis absorption spectra corresponding to the synthesized ZnO powders.

where K = 0.9; λ is the wavelength of the incident X-rays (which for this case λ = 1.5402 Å), β the width of each peak of the diffractogram at a medium height (in radians) and Θ the angle of refraction. The results of the calculations, using Eq. (3) for the most prominent peaks in Fig. 1(b), are indicated in Table 2.

Observing the values indicated in Table 2, it can be concluded that the crystallite size value is different depending on the crystallographic direction considered, which indicates that the crystallite was asymmetric, that is, it presented different deformations in different crystallographic directions.

3.2.2. IR and UV–Vis spectroscopy

In Fig. 1(c) the IR spectrum of the synthesized ZnO is shown. In the spectrum, different bands are observed, corresponding to different functional groups, featuring in particular a small band located between 3200 and 3500 cm^{-1} that is associated with the OH groups present in the sample (O–H stretching vibration mode). Another band located at ~2340 cm^{-1} would correspond to the CO_2 adsorbed from the environment and the one found at 1628 cm^{-1} is associated with a vibrational mode of water (flexion of the H–O–H functional group) (Socrates, 2001). Undoubtedly, the band most evident in the diffractogram is located at ~443 cm^{-1} - the band characteristic of ZnO (Rodríguez-Páez et al., 2001).

Meanwhile, in Fig. 1(d) the UV–Vis absorption spectra corresponding to two concentrations of suspensions of the synthesized ZnO are shown. They show an absorption maximum at λ ~385 nm (corresponding to an energy value of ~3.25 eV) and that would be related to electronic transitions from the valence band to the conduction band. The corresponding energy value, associated with this electronic transition, is related to the value of the band gap width and that in the scientific literature is reported with a value of ~3.4 eV. Since the absorption edge falls smoothly, above the maximum, there is cause to anticipate electronic transitions involving defects (West, 1984). The electronic transitions below the absorption maximum (λ < 385 nm) would be associated with transitions that would involve localized states corresponding to the Zn^{2+} and O^{2-} ions (charge transfer spectrum).

3.2.3. Scanning electron microscopy and EDS spectrum

In Fig. 2(a) two photographs (at two different magnifications) taken from a powder sample of ZnO are shown. In them, the presence of small spheroidal primary particles (less than 100 nm) forming the soft agglomerates observed there is evident. The EDS spectrum taken from a small region of these photographs (Fig. 2(b)) indicates that the elements that predominate are Zn and O. Looking carefully at the % of atoms reported by the elemental analysis, there would be more Zn than O atoms, indicating that the predominant defect in the sample would be the oxygen vacancies that, according to the UV–Vis absorbance spectrum, would be ionized and would propitiate the corresponding electronic transitions to values of λ > 385 nm (Fig. 1(d)).

Table 2
Crystallite size of ZnO samples synthesized by controlled precipitation using water as solvent.

Sample	ɵ (deg)	d (Å)	(hkl)
ZnO	15.954	314.381	(100)
	17.283	358.774	(002)
	18.187	360.590	(101)
	15.977	232.395	(100)
	17.329	256.332	(002)
	18.210	235.198	(101)
	15.977	314.418	(100)
	17.306	358.820	(002)
	18.210	208.060	(101)

3.3. Study of glyphosate removal by ZnO-NPs

3.3.1. Calibration curve

Fig. 3 shows the UV–Vis absorption spectra corresponding to different concentrations of glyphosate, between 250 and 5000 ppm (Fig. 3(a)), and the corresponding absorbance values of the maximum characteristic of the herbicide (λ = 193 nm), for the different concentrations used (calibration curve - Fig. 3(b)).

The UV–Vis spectra in Fig. 3(a) indicate that glyphosate exhibited several absorption maxima for concentrations greater than 2000 ppm (193, 200 and 205 nm) while for concentrations less than or equal to 1000 ppm, only 193 nm appears. The absorption value of the maximum located at 193 nm, obtained for each of the solutions evaluated, was plotted based on the glyphosate concentrations, between 250 and 5000 ppm, obtaining the calibration curve (Fig. 3(b)). As can be seen in Fig. 3(b), there is a substantially linear behavior (R^2 = 0.972) between the absorbance value of this maximum and the glyphosate concentration, within this interval.

3.3.2. Effect of different concentrations of ZnO-NPs on aqueous glyphosate solutions

Fig. 4 shows the UV–Vis absorption spectra corresponding to aliquots of glyphosate solutions with equal concentrations of herbicide and ZnO-NPs, taken every 10 min for 1 h. The most notable behavior of the spectra in Fig. 4, independently of the concentration ratio, is that the intensity of the maximum is reduced appreciably and that the location of this band moves slightly towards higher λ values. This result indicates, according to the calibration curve obtained (Fig. 3(b)), that the concentration of glyphosate in the solution was appreciably reduced by the presence of the nanoparticles.

To obtain more information about the effect of the presence of the ZnO-NPs on the aqueous solutions of the herbicide, other glyphosate-ZnO-NP concentration ratios were considered: (a) 700 ppm–250 ppm (Fig. 5(a)), (b) 1000 ppm–250 ppm (Fig. 5(b)) and (c) 1000 ppm–700 ppm (Fig. 5(c)), respectively, the oxide content being lower. Similarly, aliquots of the suspension were taken periodically, every 10 min for 1 h. It is noteworthy in Fig. 5 that, although the ZnO-NP content was lower than the glyphosate concentration, there was always a very good effect of removal of the herbicide by the nanoparticles. Additionally, in the spectra in Fig. 5 the displacement of this band was also evident towards higher λ values, as well as the appearance of other small absorption bands. These results would indicate the efficient removal of glyphosate from the solution due to the presence of the ZnO-NPs, as well as the possible generation of new compounds, derived from glyphosate, which would present different absorption maxima close to the characteristic band of the herbicide (193 nm).

3.3.3. C/C_o and % removal curves obtained for glyphosate solutions subjected to the action of nanoparticles

To obtain quantitative information on the process of removal of glyphosate from the designed aqueous solutions subjected to the action of the ZnO-NPs synthesized in this work, using the experimental data obtained from Figs. 4 and 5 and using the calibration curve (Fig. 3(b)), the C/Co and % removal ((C_o–C)/C_o)x100%) curves were plotted as a function of time (Fig. 6), where C_o is the initial concentration of glyphosate and C the concentration of the herbicide for a time t in the solution.

Looking at the curves in Fig. 6, the strong effect of glyphosate removal by the ZnO-NPs is reiterated. To make this effect evident, Table 3 was constructed using the maximum removal values corresponding to the different glyphosate-ZnO-NP concentration ratios evaluated. This table indicates that the percent removal of the herbicide by the nanoparticles showed a low value, between 69 and 72%, for glyphosate-ZnO-NP ratios of 700 ppm–700 ppm and 1000 ppm–1000 ppm respectively, and a maximum value for the 1000 ppm–

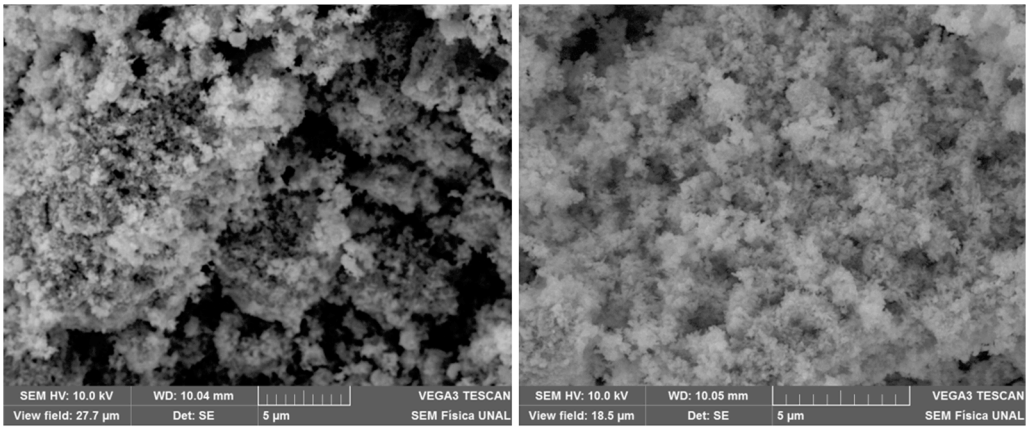

(a)

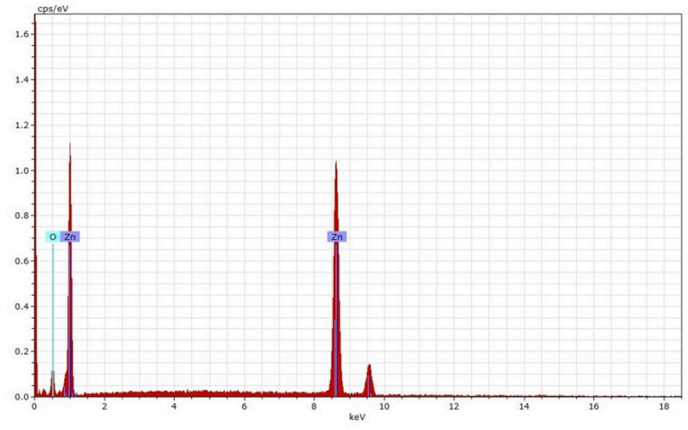

Spectrum: AM8 3652

El	AN	Series	unn. C [wt.%]	norm. C [wt.%]	Atom. C [at.%]	Error (1 Sigma) [wt.%]
Zn	30	K-series	73.72	85.48	59.03	1.95
O	8	K-series	12.52	14.52	40.97	3.20
		Total:	86.24	100.00	100.00	

(b)

Fig. 2. Photographs taken with SEM (a) and EDS spectrum (b) corresponding to the synthesized ZnO powders.

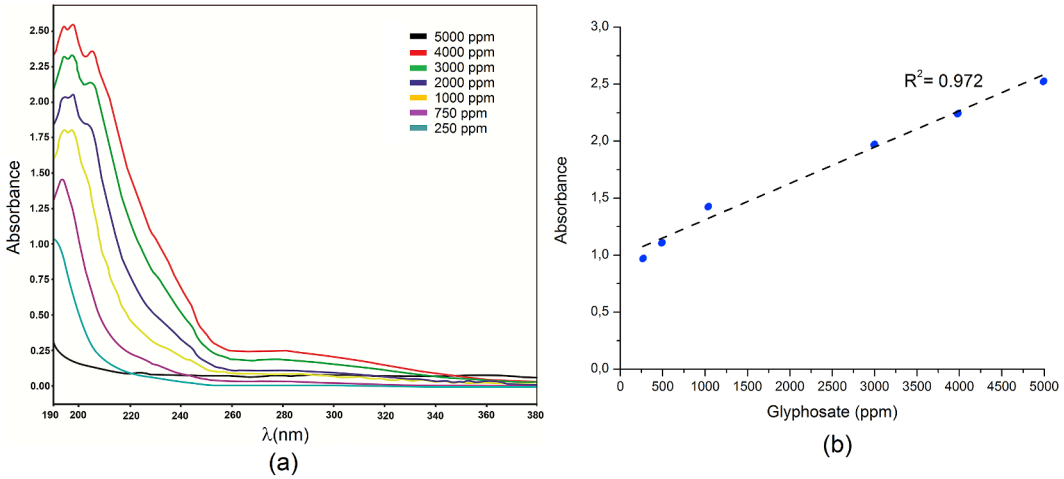

Fig. 3. (a) UV–Vis absorption spectra of different glyphosate concentrations (ranging between 1000 and 5000 ppm) and (b) absorbance values corresponding to the characteristic band of maximum absorption of glyphosate (193 nm) for the different concentrations used (calibration curve).

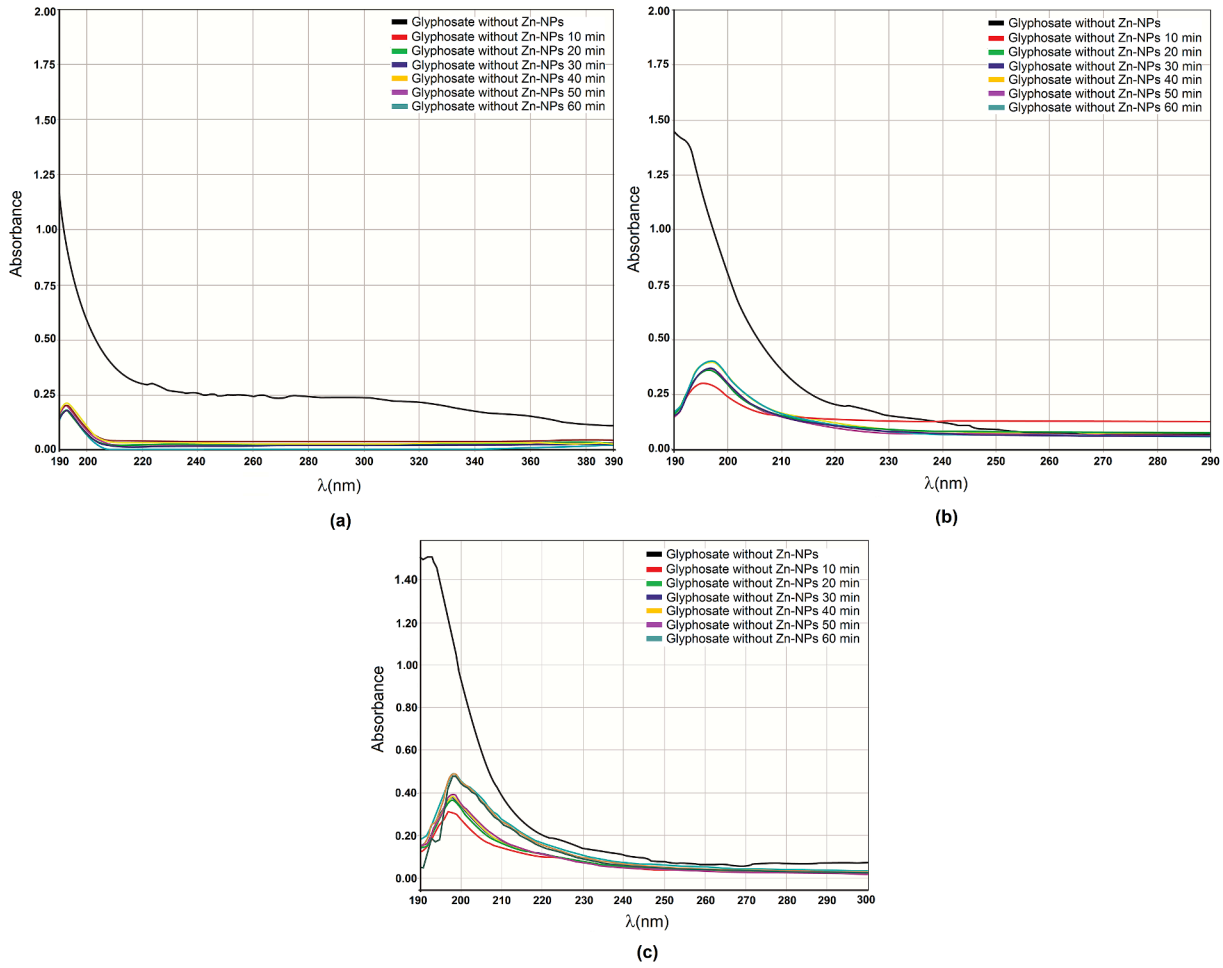

Fig. 4. UV–Vis absorbance spectra as a function of the removal time corresponding to aliquots of the following glyphosate-ZnO-NP concentrations: (a) 250 ppm–250 ppm, (b) 700 ppm–700 ppm and (c) 1000 ppm–1000 ppm, taken every 10 min during the test.

250 ppm system. It should be indicated that, as can be seen in Table 3, the tests were performed with a concentration of ZnO-NPs less than or similar to that of glyphosate, considering the efficiency of the process (lower oxide yield synthesized compared to a high concentration of herbicide).

3.3.4. Evaluation of the kinetics of glyphosate removal by ZnO-NPs

To obtain more information about the process of glyphosate removal by the ZnO-NPs, the data in Fig. 6 were used, specifically those indicated in the C/C_o curves, i.e. the different values of C in the different instants of the test in which the spectra were taken. Using these values and considering the different possible kinetics of the process (Ramesh et al., 2014; Yagub et al., 2014): pseudo first order ($\log (q_e - q) = \log q_e - (K_1 t)/2.303$), pseudo second order ($t/q = 1/(k_2 q_e^2) + t/q_e$, when the chemisorption process predominates) and intraparticle diffusion ($q = k_p t^{1/2} + cte$), with $q_e = (C_o - C_e)V/W$ and $q = (C_o - C)V/W$ and with C_o being the initial concentration of glyphosate (ppm), C the concentration of the herbicide at time t (in ppm) and C_e the concentration at equilibrium (ppm), V the volume of the solution and W the weight of the ZnO-NPs used, the curves of Fig. 7 were obtained (we considered the proportionality of q_e with $(C_o - C_e)$ and q with $(C_o - C)$ to actually graph the curves in terms of concentrations rather than in those of the q parameters). The curves of -log (C/Co) and t/C vs time, as well as C vs $time^{1/2}$, for aqueous solutions with different glyphosate-ZnO-NP concentration ratios, are indicated in Fig. 7.

Observing the curves in Fig. 7, the kinetics of the physicochemical processes that occurred within the solutions with glyphosate-ZnO-NP concentrations of 250 ppm–250 ppm (Fig. 7(i)), 700 ppm–700 ppm (Fig. 7(ii)), 1000 ppm–1000 ppm (Fig. 7(iii)) and 1000 ppm–700 ppm (Fig. 7(v)) were of pseudo second order, where chemisorption would predominate, while for the solution with 1000 ppm–250 ppm ratio (Fig. 7(iv)) the order of its kinetics could not be determined. As a result of the data obtained, the intra-particle diffusive contribution to the process could not be disregarded, especially for the solutions with 1000 ppm–250 ppm (Fig. 7(iv)) and 1000 ppm–700 ppm (Fig. 7(v)) which contained the highest concentration of glyphosate.

Looking at the two important phenomena that can occur during the removal of glyphosate by the action of ZnO-NPs - adsorption and degradation of the herbicide - it can be concluded based on the results that adsorption was predominant. This result can be accounted for considering the small particle size of the synthesized ZnO (Fig. 2(a) and Table 2) that ought to favor a high specific surface area. While in the UV–Vis absorption spectra corresponding to different glyphosate-ZnO-NP concentrations and in different instants of the trial (Figs. 4 and 5) slight deviations of the absorption maximum and the appearance of other apparent absorption bands are observed, with the study techniques used, the development of chemical reactions leading to the degradation of glyphosate could not be demonstrated.

To conduct a fuller discussion of the results obtained in this study, it is worth remembering that there is a huge interest in cleaning up aqueous solutions contaminated with glyphosate (Pankajakshan et al., 2018; Zhou et al., 2017; Balci et al., 2009). Previous work has led to details of the metabolism and degradation of glyphosate in soil and

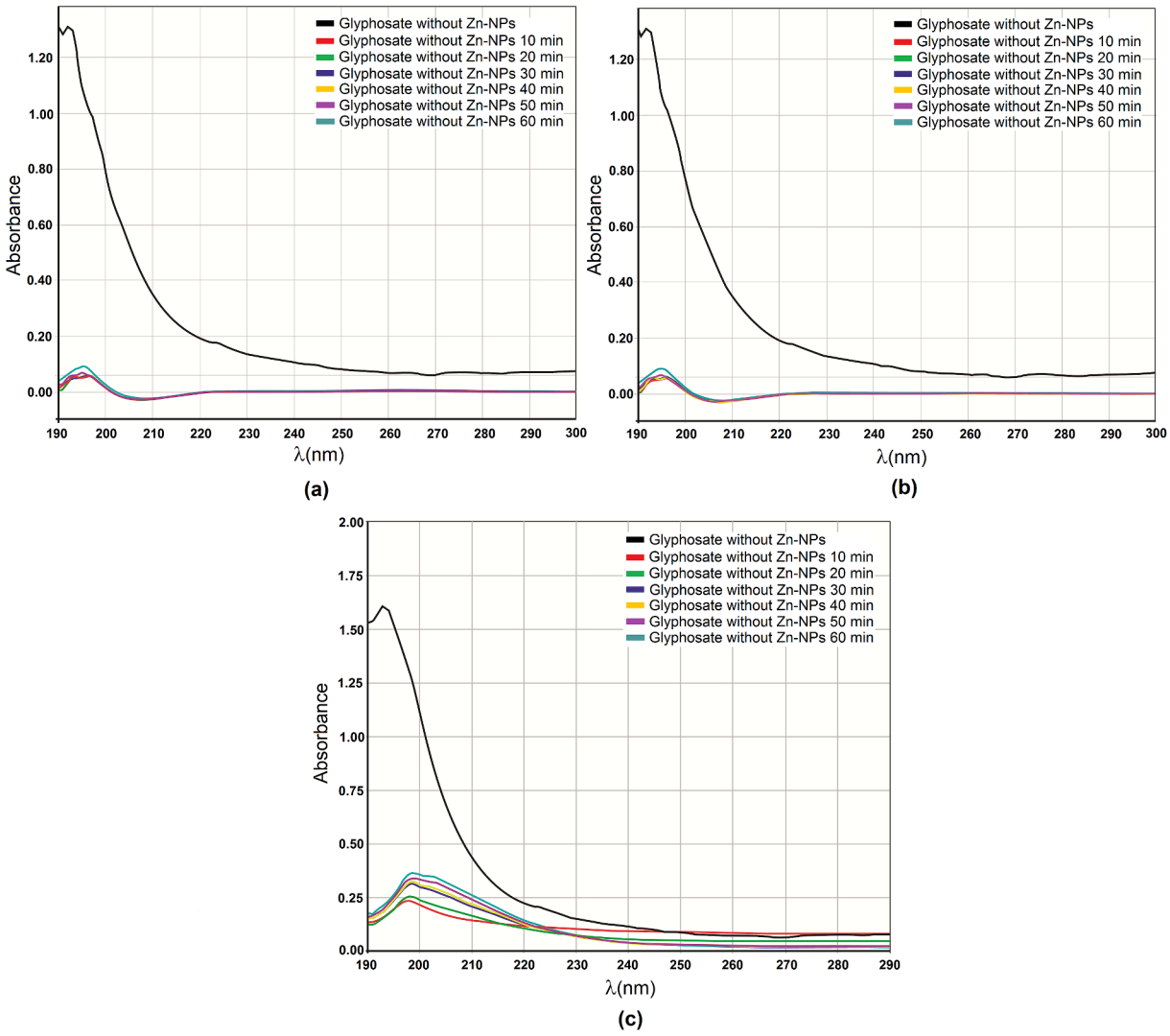

Fig. 5. UV–Vis absorption spectra corresponding to aliquots of aqueous solutions of the herbicide subjected to the action of the synthesized nanoparticles, considering different glyphosate-ZnO-NP concentrations: (a) 700 ppm–250 ppm, (b) 1000 ppm–250 ppm and (c) 1000 ppm–700 ppm, taken every 10 min during the test.

water (Dollinger et al., 2015; Rueppel et al., 1977), results that have made it possible to determine the effect of polycations, which exist in these media, on the mineralization of the herbicide (Dollinger et al., 2015; Ololade et al., 2014; Kobylecka et al., 2000; Caetano et al., 2012; Kim et al., 2011; Sundaram and Sundaram, 1997), specifically to define a glyphosate degradation pathway (Catao and López-Castillo, 2018) and the deprotonation reactions of the agrochemical (Li et al., 2018; Liu et al., 2016). The results obtained in these studies indicate that, since glyphosate has three polar functional groups (amine, carboxylate and phosphonate), it may be linked to polyvalent metal cations showing a special chelating characteristic of the herbicide (Mertens et al., 2018). Several mechanisms have been proposed to account for the sorption of glyphosate by soil and sediments that would involve the formation of strong M–OH–P (glyphosate) bonds by ligand exchange between the glyphosate phosphonate group and single coordinated M-OH groups of the surface of the minerals contained in the soil (Ololade et al., 2014; Borggaard and Gimsing, 2008; Dideriksen and Stipp, 2003). In addition, complexes that would form between the glyphosate phosphonate groups and soil-exchanged polycovalent cations would be responsible for the strong sorption of glyphosate by the soil. Bearing this in mind, a series of studies were carried out that evaluate the formation of cation-glyphosate complexes for different cations, thereby determining which of them is more favorable to the herbicide forming complexes, while advancing understanding of the process of inactivation of organophosphorus herbicides (Caetano et al., 2012; Sundaram et al., 1997; Cotinho and Mazo, 2005). Taking into account the specific interactions between the metals in the soil and glyphosate, the low activity of the herbicide when applied directly inside the ground and not pulverized can be understood, as well as the possible processes for its degradation. The glyphosate (polyprotic acid) can act as a chelating agent and form stable complexes with divalent and trivalent metal cations (Caetano et al., 2012; Cotinho et al., 2005; Subramaniam and Hoggard, 1988; Motekaitis and Martell, 1985). The calculations of free energy of complexation between glyphosate and some divalent and trivalent cations, carried out in the work of Caetano et al. (2012) in coordinated octahedral and tetrahedral environments, showed that the three most stable complexes would be formed by the herbicide with Zn^{2+}, Cu^{2+} and Co^{3+}. Specifically, glyphosate-Zn is 14.72 kcal/mol more stable than glyphosate-Cu, which is 24.42 kcal/mol more stable than glyphosate-Co. In conclusion, the order of stability of the complexes the glyphosate would form with some cations, in aqueous medium, would be: Zn > Cu > Co > Fe > Cr > Al > Ca > Mg, according to Caetano et al. (2012). These results indicate that a favorable route to inactivate glyphosate would be to use solid systems rich in Zn^{2+} and/or Cu^{2+}, as in the present work, where ZnO was used.

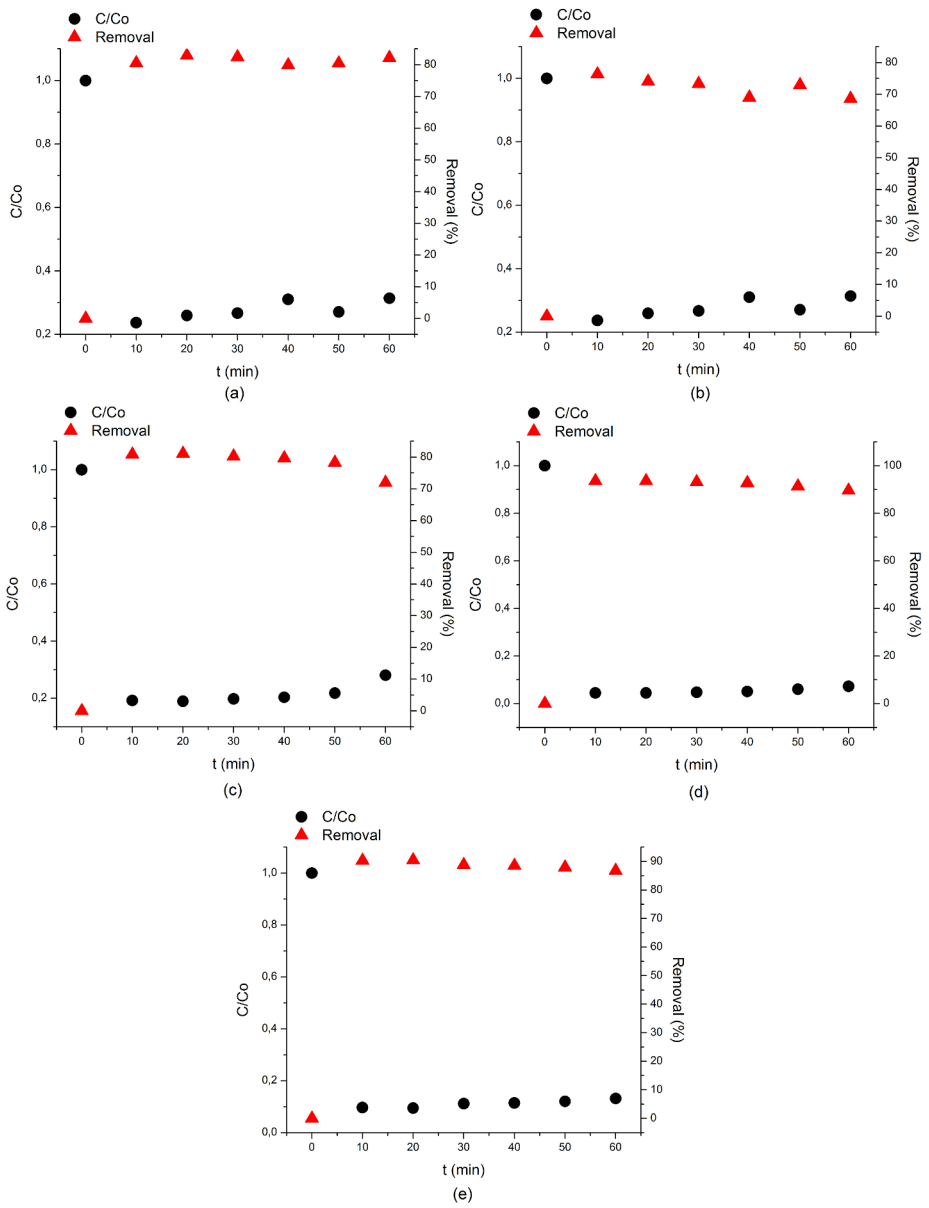

Fig. 6. C/C_o and glyphosate % removal $((C_o–C)/C_o)$ curves as a function of time for different glyphosate-ZnO-NP concentrations: (a) 250 ppm–250 ppm, (b) 700 ppm–700 ppm, (c) 1000 ppm–1000 ppm, (d) 1000 ppm–250 ppm and (e) 1000 ppm-700 ppm.

Table 3
Percentages of glyphosate removal by the synthesized ZnO-NPs.

Roundup (ppm)	ZnO (ppm)		
	250	700	1000
250	80%	–	90%
700	–	69%	87%
1000	–	–	72%

Considering the results (Figs. 4–7) alongside the above observations, an important step in the evident removal of glyphosate by ZnO-NPs would be the adsorption of the herbicide on the surface of NPs. As occurs in other systems (Borggaard and Gimsing, 2008; Dideriksen and Stipp, 2003), glyphosate is only sorbed on surfaces of variable and poorly ordered charge, characteristic of the surfaces of the NPs, and among them those of ZnO (Baer et al., 2010, 2013; Kim et al., 2014; Ton-That et al., 2008). As with other systems (Borggaard and Gimsing, 2008; Dideriksen and Stipp, 2003; Sheals et al., 2002), sorption of glyphosate on ZnO-NPs might occur by ligand exchange or specific sorption, favoring the formation of monodentate surface complexes at singly-coordinated hydroxyl groups (mononuclear species), although the formation of bidentate (bridging) surface complexes and contiguous (neighboring) singly coordinated hydroxyl groups (surface binuclear species) cannot be ruled out. The formation of these complexes on the surface of the ZnO-NPs is illustrated in Fig. 8.

Another possibility is that the carboxyl group binds to the surface of the NPs but, as indicated by work in other systems (Sheals et al., 2002; Barja and Dos Santos, 2005), if the surface-carboxyl bond was formed, it would be very weak.

The model proposed for the adsorption of glyphosate (Fig. 8) would account for the removal of glyphosate by the ZnO-NPs and therefore the results shown in Figs. 4–6. A more careful study, using ATR-FTIR, X-ray photoelectron spectroscopy (XPS) and atomic force microscopy should be done in the future to find out more about the removal process and validate the model. Furthermore, in considering the possibility of degradation of glyphosate by ZnO-NPs, which cannot be evidenced by the results obtained in this work, we should consider the dissociation of ZnO, i.e. the generation of Zn^{2+} ions with

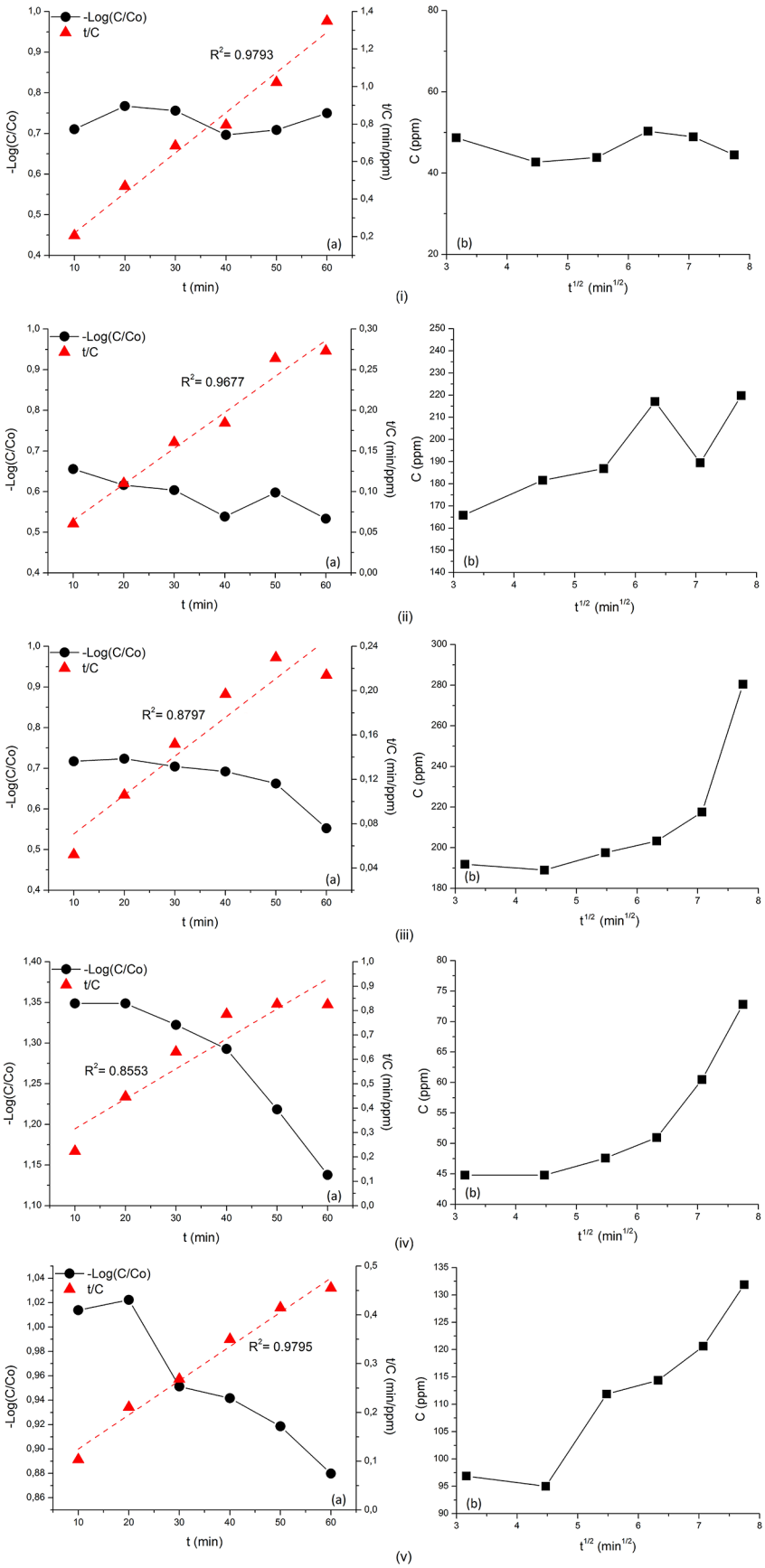

Fig. 7. Curves for (a) -log (C/Co) vs time and t/C vs time, and (b) C vs time$^{1/2}$ for aqueous solutions with different glyphosate-ZnO-NP concentration ratios: (i) 250 ppm–250 ppm, (ii) 700 ppm–700 ppm, (iii) 1000 ppm–1000 ppm ZnO, (iv) 1000 ppm–250 ppm and (v) 1000 ppm–700 ppm, respectively.

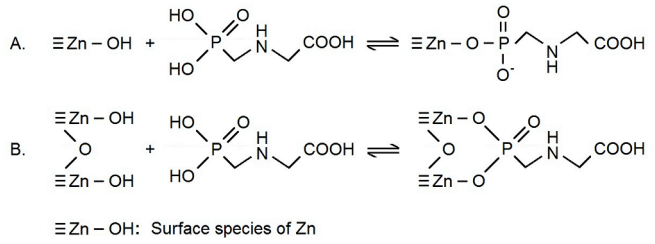

Fig. 8. Proposed model for adsorption of glyphosate on the surface of ZnO-NPs.

which the glyphosate could form complexes (Kobylecka et al., 2000; Caetano et al., 2012; Kim et al., 2011), as well as the formation of reactive oxygen species (ROS) mediated by defects (Prasanna and Vijayaraghavan, 2015), that would lead to a process of degradation as indicated by Kudzin (Kudzin et al., 2019). Therefore it is necessary, in future work, to use techniques such as liquid and/or gas chromatography coupled with mass spectroscopy to identify the byproducts generated through the interaction of ZnO nanoparticles with glyphosate, to verify if degradation of the herbicide occurs.

4. Conclusions

A suitable synthesis method was structured that allowed us to obtain ZnO-NPs in a controllable way. These had a nanometric particle size (<100 nm), a spheroidal morphology and formed soft agglomerates. The nanoparticles were well crystallized with a wurtzite structure. From the results of UV–Vis absorption spectroscopy it was possible to determine that their energy gap value was ~3.25 eV. It is observed that in each of the glyphosate - ZnO-NPs combinations prepared, using different NP concentrations, there was a reduction in absorbance, which indirectly shows a decrease in the concentration of the herbicide. The evaluation trials for actions due to ZnO-NP presence in the glyphosate solutions showed an efficient removal of the herbicide, from ~70% to 90% depending on the glyphosate-ZnO-NP ratio. This would occur mainly through a chemisorption process (kinetics of a pseudo second order removal).

Declaration of competing interest

On behalf of all authors, the corresponding author J. E. Rodríguez-Páez states that there is no conflict of interest.

Acknowledgments

We are especially grateful to the Jorge Tadeo Lozano University, specifically to the instrumental laboratory, for the availability of the UV–Vis absorption spectrometer and to Technician Carol Rocío Delgado Lizarazo for her collaboration. We are also grateful to the University of Cauca for having facilitated the use of the CYTEMAC Laboratory equipment for the synthesis process. Furthermore, we are grateful to Colin McLachlan for suggestions relating to the English text.

References

Abdennouri, M., Baalala, M., Galadi, A., El Makhfouk, M., Bensitel, M., Nohair, K., Sadiq, M., Boussaoud, A., Barka, N., 2016. Photocatalytic degradation of pesticides by titanium dioxide and titanium pillared purified clays. Arabian J. Chem. 9, S313–S318. https://doi.org/10.1016/j.arabjc.2011.04.005.

Ahrens, W.H., 1994. Herbicide Handbook of the Weed Science Society of America. seventh ed. Weed Science Society of America.

Anifandis, G., Katsanaki, K., Lagodonli, G., Messini, C., Simopoulou, M., Daponte, K., 2018. The effect of glyphosate on Human sperm motility and sperm DNA fragmentation. Int. J. Environ. Res. Public Health 15, E1117. https://doi.org/10.3390/ijerph15061117.

Assalin, M.R., De Moraes, S.G., Queiroz, S.C.N., Feracini, V.L., Duran, N., 2010. Studies on degradation of glyphosate by several oxidative chemical process: ozonation, photolysis and heterogeneous photocatalysis. J. Environ. Sci. Health, Part B 45, 89–94. https://doi.org/10.1080/03601230903404598.

Baer, D.R., Engelhard, M.H., Johnson, G.E., Laskin, J., Lai, J., Mueller, K., Munusamy, P., Thevathasan, S., Wang, H., Washton, N., 2013. Surface characterization of nanomaterials and nanoparticles: important needs and challenging opportunities. J. Vac. Sci. Technol. A 31, 050820. https://doi.org/10.1116/1.4818423.

Baer, D., Gaspar, D.J., Nachimuthu, P., Techane, S.D., Castner, D.G., 2010. Application of surface chemical analysis tools for characterization of nanoparticles. Anal. Bioanal. Chem. 396, 983–1002. https://doi.org/10.1007/s00216-009-3360-1.

Balci, B., Oturan, M.A., Oturan, N., Sirés, I., 2009. Decontamination of aqueous glyphosate, (Aminomethyl) phosphonic acid, and glyphosate solutions by electro fenton-like process with Mn^{2+} as the catalyst. J. Agric. Food Chem. 57, 4888–4894. https://doi.org/10.1021/jf900876x.

Barja, B.C., Dos Santos, A.M., 2005. Aminomethyl phosphonic acid and glyphosate adsorption onto goethite: A comparative study. Environ. Sci. Technol. 39, 585–592. https://doi.org/10.1021/es035055q.

Barret, K.A., McBride, M.B., 2005. Oxidative degradation of glyphosate and aminomethylphosphonate by manganese oxide. Environ. Sci. Technol. 39, 9223–9228. https://doi.org/10.1021/es051342d.

Beecham, J.E., Seneff, S., 2015. The possible link between autism and glyphosate acting as glycine mimetic – a review of evidence from the literature with analysis. J. Mol. Genet. Med. 9, 1000197. https://doi.org/10.4172/1747-0862.1000187.

Benachour, N., Séralini, G.E., 2009. Glyphosate formulations induce apoptosis and necrosis in human umbilical, embryonic, and placental cells. Chem. Res. Toxicol. 22, 97–105. https://doi.org/10.1021/tx800218n.

Benbrook, C.M., 2016. Trends in glyphosate herbicide use in the United States and globally. Environ. Sci. Eur. 28 (3) (pp 15). https://doi.org/10.1186/s12302-016-0070-0.

Bernal, M.H., Salomon, K.R., Carrasquilla, G., 2009. Toxicity of formulated Glyphosate (Glyphos) and cosmo-flux to larval Colombian frogs 1. Laboratory acute toxicity. J. Toxicol. Environ. Health, Part A 72, 961–965. https://doi.org/10.1080/15287390902929709.

Bernal, M.H., Solomon, K.R., Carrasquilla, G., 2009. Toxicity of formulated Glyphosate (Glyphos) and cosmo-flux to larval and Juvenile Colombian frogs 2. Field and Laboratory Microcosm acute toxicity. J. Toxicol. Environ. Health, Part A 72, 966–973. https://doi.org/10.1080/15287390902929717.

Borggaard, O.K., Gimsing, A.L., 2008. Fate of glyphosate in soil and the possibility of leaching to ground and surface waters: A review. Pest Manag. Sci. 64, 441–456. https://doi.org/10.1002/ps.1512.

Bott, S., Tesfamariam, T., Kania, A., Eman, B., Aslan, N., Römheld, V., Neumann, G., 2011. Phytotoxicity of glyphosate soil residues re-mobilised by phosphate fertilisation. Plant Soil 342 (1), 249–263. https://doi.org/10.1007/s11104-010-0689-3.

Burchfield, S.L., Bailey, D.C., Todt, C.E., Denney, R.D., Negga, R., Fitsanakis, V.A., 2019. Acute exposure to a glyphosate-containing herbicide formulation inhibits complex II and increases hydrogen peroxide in the model organism caenorhabditis elegans. Environ. Toxicol. Pharmacol. 66, 36–42. https://doi.org/10.1016/j.etap.2018.12.019.

Caetano, M.S., Ramalho, T.C., Botrel, D.F., da Cunha, E.F.F., Carvalho de Mello, W., 2012. Understanding to inactivation process f organophosphorus herbicides: A DFT study of glyphosate metallic complexes with Zn^{2+}, Ca^{2+}, Mg^{2+}, Cu^{2+}, Co^{3+}, Fe^{3+}, Cr^{3+} and Al^{3+}. Int. J. Quantum Chem. 112, 2752–2762. https://doi.org/10.1002/qua.23222.

Camacho, A., Mejía, D., 2017. The health consequences of aerial spraying illicit crops; The case of Colombia. J. Health Econ. 54, 147–160. https://doi.org/10.1016/j.jhealeco.2017.04.005.

Campuzano-Cortina, C., Feijoó Fonnegra, M.L., Manzur Pineda, K., Palacio Muñoz, M., Rendón Fonnegra, J., Zapata Díaz, J.P., 2017. Efectos de la intoxicación por glifosato en la población agrícola: revisión del tema. Salud Publica (Caracas) 8 (1), 121–133.

Cao, L., Ma, D., Zhou, Z., Xu, C., Cao, C., Zhao, P., Huang, Q., 2019. Efficient photocatalytic degradation of herbicide glyphosate in water by magnetically separable a recyclable $BiOBr/Fe_3O_4$ nanocomposites under visible light irradiation. Chem. Eng. J. 368, 212–222. https://doi.org/10.1016/j.cej.2019.02.100.

Castle, L.A., Shiehl, D.L., Gorton, R., Patten, P.A., Chen, Y.H., Bertain, S., Chou, H.J., Duck, N., Wong, J., Liu, D., Lassne, r M.W., 2004. Discovery and directed evolution of a glyphosate tolerance gen. Science 304, 1151–1154. https://doi.org/10.1126/science.1096770.

Catao, A.J.L., López-Castillo, A., 2018. On the degradation pathway of glyphosate and glycine. Environ. Sci.: Processes Impacts 20, 1148–1157. https://doi.org/10.1039/c8em00119g.

Conrad, A., Schröter-Kermani, C., Hoppe, H.W., Rüther, M., Pieper, S., Kolossa-Gehring, M., 2017. Glyphosate in German adults – Time trend (2001 to 2015) of human exposure to a widely used herbicide. Int. J. Hyg Environ. Health 220 (1), 8–16. https://doi.org/10.1016/j.ijheh.2016.09.016.

Cotinho, C.F.B., Mazo, L.H., 2005. Complexos metálicos com o herbicida glifosato: Revisao. Quim. Nova 28, 1038–1045. https://doi.org/10.1590/S0100-40422005000600019.

Dai, P., Hu, P., Tang, J., Li, Y., Li, C., 2016. Effect of glyphosate on reproductive organs in male rat. Acta Histochem. 118, 519–526. https://doi.org/10.1016/j.acthis.2016.05.009.

Dallegrave, E., Mantese, F., Oliveira, R., Andrade, A., Dalsenter, P., Langeloh, A., 2007. Pre- and postnatal toxicity of the commercial glyphosate formulation in Wistar rats. Arch. Toxicol. 81 (9), 665–673. https://doi.org/10.1007/s00204-006-0170-5.

Damalas, C.A., Elefthero Horinos, I.G., 2011. Pesticide exposure, safety issues, and risk

assessment indicators. Int. J. Environ. Res. Public Health 8, 1402–1419. https://doi.org/10.3390/ijerph8051402.
Dideriksen, K., Stipp, S.L.S., 2003. The adsorption of glyphosate and phosphate to goethite: A molecular-scale atomic force microscopy study. Geochem. Cosmochim. Acta 67, 3313–3327. https://doi.org/10.1016/S0016-7037(02)01369-8.
Dollinger, J., Dagés, C., Voltz, M., 2015. Glyphosate sorption to soils and sediments predicted by pedotransfer functions. Environ. Chem. Lett. 13, 293–307. https://doi.org/10.1007/s10311-015-0515-5.
Goldsborough, L.G., Beck, A.E., 1989. Rapid dissipation of glyphosate in small forest ponds. Arch. Environ. Contam. Toxicol. 18, 537–544. https://doi.org/10.1007/BF01055020.
González-Martínez, M.A., Brun, E.M., Puchades, R., Maquieire, A., Ramsay, K., Rubio, F., 2005. Glyphosate immunosensor. Application for water and soil analysis. Anal. Chem. 77, 4219–4227. https://doi.org/10.1021/ac048431d.
Grillion, R.J., Barbash, J.E., Kolpin, D.W., Larson, S.J., 1999. Peer reviewed: Testing water quality for pesticide pollution. Environ. Sci. Technol. 33, 164A-169A. https://doi.org/10.1021/es992770k.
Gui, Y.X., Fan, N.X., Wang, H.M., Wang, G., Chen, S., 2012. Glyphosate induced cell death through apoptotic and autophagic mechanisms. Neurotoxicol. Teratol. 34, 344–349. https://doi.org/10.1016/j.ntt.2012.03.005.
Huo, R., Yang, L., Liu, Y.Q., Xu, Y.H., 2017. Visible-light photocatalytic degradation of glyphosate over $BiVO_4$ prepared by different coprecipitation methods. Mater. Res. Bull. 88, 56–61. https://doi.org/10.1016/j.materresbull.2016.12.012.
Jaisi, D.P., Li, H., Wallece, A.F., Paudel, P., Sun, M., Balakrishra, A., Lerch, B.N., 2016. Mechanism of bond cleavage during Mn oxide and UV degradation of glyphosate: results from oxygen isotopes and molecular simulations. J. Agric. Food Chem. 64, 8474–8483. https://doi.org/10.1021/acs.jafc.6b02608.
Jayasumana, C., Gunatilake, S., Senanayake, P., 2014. Glyphosate, hard water and nephrotoxic metals: are they the culprits behind the epidemic of chronic kidney disease of unknown etiology in Sri Lanka?. Int. J. Environ. Res. Public Health 11, 2125–2147. https://doi.org/10.3390/ijerph110202125.
Keum, Y.S., Li, X.Q., 2004. Reduction of nitroaromatic pesticides with zero-valent iron. Chemosphere 54, 255–263. https://doi.org/10.1016/j.chemosphere.2003.08.003.
Khatri, N., Tyagi, S., Rawtani, D., 2016. Assessment of drinking water quality and its health effects in rural áreas of Harij taluka, Patan district of northern Gujarat. Environ. Claims J. 28, 223–246. https://doi.org/10.1080/10406026.2016.1190249.
Kim, K.M., Choi, M.H., Lee, J.K., Jeong, J., Kim, Y.R., Kim, M.K., Paek, S.M., Oh, J.M., 2014. Physicochemical properties of surface charge-modified ZnO nanoparticles with different particles sizes. Int. J. Nanomed. 9 (Suppl. 2), 41–56. https://doi.org/10.2147/IJN.S57923.
Kim, B., Kim, Y.S., Hay, A.G., McBride, M.B., 2011. Effect of soil metal contamination of glyphosate mineralization: Role of zinc in the mineralization rates of two copper-spiked mineral soils. Environ. Toxicol. Chem. 30, 596–601. https://doi.org/10.1002/etc.424.Epub.2011.
Kobylecka, J., Ptaszynski, B., Zwolinska, A., 2000. Synthesis and properties of complexes of lead(II), cadmium(II), and zinc(II) with N-phosphonomethyl glycine. Monatshefte Chem. 131, 1–11. https://doi.org/10.1007/s007060050001.
Kudzin, M.H., Zylla, R., Mrozinska, Z., Urbaniak, P., 2019. ^{31}P NMR investigations on Roundup degradation by AOP procedures. Water 11, 331. https://doi.org/10.3390/w11020331.
Lan, H., Jiao, Z., Zhao, X., He, W., Wang, A., Liu, H., Liu, R., Qu, J., 2013. Removal of glyphosate from water by electrochemically assisted MnO_2 oxidation process. Separ. Purif. Technol. 117, 30–34. https://doi.org/10.1016/j.seppur.2013.04.012.
Li, Q., Liu, B., Mu, W., Yu, Q., Tian, Y., Liu, G., Yang, Y., Li, X., Luo, S., 2018. Protonation states of glyphosate in aqueous solution. J. Solut. Chem. 47, 705–714. https://doi.org/10.1007/s10953-018-0751-y.
Li, J., Smeda, R.J., Sellers, B.A., Johnson, W.G., 2005. Influence of formulation and glyphosate salt on absorption and translocation in three annual weeds. Weed Sci. 53, 153–159. https://doi.org/10.1614/WS-03-075R1.
Liu, B., Dong, L., Yu, Q., Li, X., Wu, F., Tan, Z., Luo, S., 2016. Thermodynamic study on the protonation reactions of glyphosate in aqueous solution: Potentiometry, calorimetry and NMR spectroscopy. J. Phys. Chem. B 120, 2132–2137. https://doi.org/10.1021/acs.jpcb.5b11550.
Manassero, C., Passalia, C., Negro, A.C., Cassaro, A.E., Zalazar, C.S., 2010. Glyphosate degradation in water employing the H_2O_2/UVC process. Water Res. 44, 3375–3882. https://doi.org/10.1016/j.watres.2010.05.004Mann.
Mann, R.M., Bidwell, J.R., 1999. The Toxicity of glyphosate and several glyphosate formulations to four species of southwestern Australian frogs. Arch. Environ. Contam. Toxicol. 36 (2), 193–199. https://doi.org/10.1007/s002449900460.
Méndez-Villaquirán, A.F., 2015. Aislamiento e identificación de bacterias capaces de degradar glifosato. Universidad ICESI, Facultad de Ciencias Naturales, Departamento Ciencias Química - Programa Química Farmacéutica, Santiago de Cali – Colombia.
Mertens, M., Höss, S., Neumann, G., Afzal, J., Reichenbecher, W., 2018. Glyphosate, a chelating agent-relevant for ecological risk assessment?. Environ. Sci. Pollut. Res. Int. 25, 5298–5317. https://doi.org/10.1007/s11356-017-1080-1.
Monsanto, 2002. Risk Assessment and Risk Management Plan Final Version DIR 020/2002, Commercial Release of Roundup Ready® Canola. Accessed date:. http://www.ogtr.gov.au/internet/ogtr/publishing.nsf/Content/dir020-3/$FILE/dir020finalrarmpsum.pdf.
Monsanto, 2019. Accessed date:. http://www.monsanto.com/global/au/products/documents/tech-topic-what-is-roundup-ready-canola.pdf.
Monsanto, 2014. Backgrounder Glyphosate and Water Quality. Accessed date:. https://monsanto.com/app/uploads/2017/06/glyphosate-and-water-quality.pdf.
Moradi Dehaghi, S., Rahmanifar, B.Y., Moradi, A.M., Azar, P.A., 2014. Removal of permethrin pesticide from water by chitosan – zinc oxide particles composite as and adsorbent. J. Sau. Chem. Soc. 18, 348–355. https://doi.org/10.1016/j.jscs.2014.01.004.
Motekaitis, R.J., Martell, A.E., 1985. Metal chelate formation by N-Phosphonomethyl glycine and related ligands. J. Coord. Chem. 14, 139–149. https://doi.org/10.1080/00958978508073900.
Nasrabadi, T., Bidhendi, G.N., Karbassi, A., Grathwohl, P., Mehrdadi, N., 2011. Impact of major organophosphate pesticides used in agriculture to surface water and sediment quality (Southern Caspian Sea basin, Haraz River). Environ. Earth. Sci. 63, 873–883.
Navarro, S., Fenoll, J., Vela, N., Ruiz, E., Navarro, G., 2009. Photocatalytic degradation of eight pesticides in leaching water by use of ZnO under natural sunight. J. Hazard Mater. 172, 1303–1310. https://doi.org/10.1016/j.jhazmat.2009.07.137.
Ololade, J.A., Oladoja, N.A., Oloye, F.F., Alomaja, F., Akerele, D.D., Iwaye, J., Aikpokpodion, P., 2014. Sorption of glyphosate on soli components: The roles of metal oxide and organic materials. Soil Sediment Contam. 23, 571–585. https://doi.org/10.1080/15320383.2014.846900.
Pankajakshan, A., Sinha, M., Ohja, A.A., Mandal, S., 2018. Water-stable nanoscale zirconium-based metal-organic frameworks for the effective removal of glyphosate from aqueous media. ACS Omega 3, 7832–7839. https://doi.org/10.1021/acsomega.8b00921.
Plakas, K.V., Karabelas, A.J., 2012. Removal of pesticides from water by NF and RO membranes – A review. Desalination 287, 255–265. https://doi.org/10.1016/j.desal.2011.08.003.
Prasanna, V.L., Vijayaraghavan, R., 2015. Insight into the mechanism of antibacterial activity of ZnO – surface defects mediated reactive oxygen species even in dark. Langmuir 31, 9155–9162. https://doi.org/10.1021/acs.langmuir.5b02266.
Pretty, J.N., Morrison, J.I.L., Hine, R.E., 2003. Reducing food poverty by increasing agriculture sustainability in developing countries. Agric. Ecosyst. Environ. 95, 217–234. https://doi.org/10.1016/S0167-8809(02)00087-7.
Ramesh, K., Rajappa, A., Roopa, V., Nandhakumar, V., 2014. Kinetics of adsorption of vinyl sulphone red dye from aqueous solution onto commercial activated carbon. Int. J. Curr. Res. Chem. Pharm. Sci. 1 (1), 28–36.
Rawtani, D., Khatri, N., Tyagi, S., Pandey, G., 2018. Nanotechnology-based recent approaches for sensing and remediation of pesticides. J. Environ. Manag. 206, 749–762. https://doi.org/10.1016/j.jenvman.2017.11.037.
Reyes, L.C., 2014. Estimating the causal effect of forced eradication on coca cultivation in Colombian Municipalities. World Dev. 61, 70–84. https://doi.org/10.1016/j.worlddev.2014.03.024.
Rissol, R.Z., Abdalla, F.C., Costa, M.J., Rantin, F.T., Mackenzie, D.J., Kalinin, A.L., 2016. Effects of glyphosate and the glyphosate-based herbicides Roundup Original® and Roundup Transorb® on respiratory morphophysiology of bullfrog tadpoles. Chemosphere 156, 37–44. https://doi.org/10.1016/j.chemosphere.2016.04.083.
Rodríguez - Páez, J.E., Moure, C., Duran, P., Fernández, J.F., 1997. Producción de partículas de ZnO utilizando un proceso de precipitación controlada. Bol. Soc. Esp. Cerám. Vidrio 36, 136–140.
Rodríguez-Páez, J.E., Caballero, A.C., Villegas, M., Moure, C., Durán, P., Fenández, J.F., 2001. Controlled precipitation methods: formation mechanism of ZnO nanoparticles. J. Eur. Ceram. Soc. 21, 925–930. https://doi.org/10.1016/S0955-2219(00)00283-1.
Rodríguez-Páez, J.E., 2001. Síntesis de polvos cerámicos por el método de precipitación. Bol. Soc. Esp. Cerám. Vidrio 40, 173–184. https://doi.org/10.3989/cyv.2001.v40.i3.742.
Romano, R.M., Romano, M.A., Bernardi, M.M., Furtado, P.V., Oliveira, C.A., 2010. Prepubertal exposure to commercial formulation of the herbicide glyphosate alters testosterone levels and testicular morphology. Arch. Toxicol. 84 (4), 309–317. https://doi.org/10.1007/s00204-009-0494-z.
Rueppel, M.L., Brightwell, B.B., Schaefer, J., Marvel, J.T., 1977. Metabolism and degradation of glyphosate in soil and water. J. Agric. Food Chem. 25 (3), 517–528. https://doi.org/10.1021/jf60211a018.
Samsel, A., Seneff, S., 2013. Glyphosate's suppression of cytochrome P450 enzymes and amino acid biosynthesis by the gut microbiome: pathways to modern diseases. Entropy 15, 1416–1463. https://doi.org/10.3390/e15041416.
Sheals, J., Sjöberg, S., Persson, P., 2002. Adsorption of glyphosate on goethite: molecular characterization of surfaces complexes. Environ. Sci. Technol. 36, 3090–3095. https://doi.org/10.1021/es010295w.
Shifu, C., Yunzhang, L., 2007. Study on the photocatalytic degradation of glyphosate by TiO_2 photocatalyst. Chemosphere 67, 1010–1017. https://doi.org/10.1016/j.chemosphere.2006.10.054.
Socrates, G., 2001. Infrared and Raman Characteristic Group Frequencies. third ed. John Wiley & Sons Ltd., New York.
Solomon, K.R., Marshall, E.J.P., Carrasquilla, G., 2009. Human health and environmental risks from the use of Glyphosate formulations to control the production of coca in Colombia: overview and conclusions. J. Toxicol. Environ. Health, Part A 72, 914–920. https://doi.org/10.1080/15287390902929659.
Subramaniam, V., Hoggard, P.E., 1988. Metal complexes of glyphosate. J. Agric. Food Chem. 36, 1326–1329. https://doi.org/10.1021/jf00084a050.
Sundaram, A., Sundaram, K.M., 1997. Solubility products of six methalglyphosate complexes in water and forestry soils, and their influence on glyphosate toxicity to plants. J. Environ. Sci. Health, B 32, 583–598. https://doi.org/10.1080/03601239709373104.
Taghizade Firozjaee, J., Mehrdadi, N., Baghdadi, M., Nabi, Bidhendi, G.R., 2018. Application of nanotechnology in pesticides removal from aqueous solutions – A review. Int. J. Nanosci. Nanotechnol. 14, 43–56.
Tarazona, J.V., Court-Marques, D., Tiramani, M., Reich, H., Pfeil, R., Istace, F., Crivellente, F., 2017. Glyphosate toxicity and carcinogenicity: a review of the scientific basis of the European Union assessment and its differences with IARC.

Arch. Toxicol. 91, 2723–2743. https://doi.org/10.1007/s00204-017-1962-5.
Tittonell, P., 2014. Ecological intensification of agriculture – sustainable by nature. Curr. Opinion Environ. Sustain. 8, 53–61. https://doi.org/10.1016/j.cosust.2014.08.006.
Ton-That, C., Phillips, M.R., Foley, M., Moody, S.J., Stampfl, A.P.J., 2008. Appl. Phys. Lett. 92, 261916. https://doi.org/10.1063/1.2952955.
Tovakkoli, H., Yazdanbakhsh, M., 2013. Fabrication of the perovskite-type oxide nanoparticles as the new adsorbents in efficient removal of a pesticide from aqueous solutions: kinetic, thermodynamic, and adsorptions studies. Microporous Mesoporous Mater. 176, 86–94. https://doi.org/10.1016/j.micromeso.2013.03.043.
Tsui, M.T.K., Chu, L.M., 2003. Aquatic toxicity of glyphosate-based formulations: comparison between different organisms and the effects of environmental factors. Chemosphere 52, 1189–1197. https://doi.org/10.1016/S0045-6535(03)00306-0.
Umar, K., Aris, A., Ahmad, H., Parveen, T., Jaafar, J., Majid, Z.A., Reddy, A.V.B., Talib, J., 2016. Synthesis of visible light active doped TiO_2 for the degradation of organic pollutants-methylene blue and glyphosate. J. Anal. Sci. Techn. 7, 29. https://doi.org/10.1186/s40543-016-0109-2.
Valle, A.L., Mello, F.C.C., Alves-Balvedi, R.P., Rodrigues, L.P., Goulard, L.R., 2019. Glyphosate detection: methods, needs and challenges. Environ. Chem. Lett. 17, 291–317. https://doi.org/10.1007/s10311-018-0789-5.
Van Bruggen, A.H.C., He, M.M., Shin, K., Mai, V., Jeong, K.C., Finckh, M.R., Morris, J. G., 2018. Environmental and health effects of the herbicide glyphosate. Sci. Total Environ. 616–617, 255–268. https://doi.org/10.1016/j.scitotenv.2017.10.309.
Van der Bruggen, B., Schaep, J., Maes, W., Wilms, D., van de Casteele, C., 1998. Nanofiltration as a treatment method for the removal of pesticides from ground waters. Desalination 117, 139–147. https://doi.org/10.1016/S0011-9164(98)00081-2.
Vandenberg, L.N., Blumberg, B., Antoniou, M.N., Benbrook, C.M., Carroll, L., Colborn, T., Everett, L.G., Hansen, M., Landrigan, P.J., Lanphear, B.P., Mesnage, R., Vom Saal, F.S., Welshons, W.V., Myers, J.P., 2017. Is the time to reassess current safety standard for glyphosate-based herbicides?. J. Epidemiol. Community Health 71, 613–618. https://doi.org/10.1136/jech-2016-208463.
Wang, M., Zhang, G., Qiu, G., Cai, D., Wu, Z., 2016. Degradation of herbicide (glyphosate) using sunlight-sensitive MnO_2/C catalyst immediately fabricated by high energy electron beam. Chem. Eng. J. 306, 693–703. https://doi.org/10.1016/j.cej.2016.07.063.
Wang, T., Ren, J., Qu, G., Liang, D., Hu, S., 2016. Glyphosate contaminated soil remediation by atmospheric pressure dielectric barrier discharge plasma and its residual toxicity evaluation. J. Hazard Mater. 320, 539–546. https://doi.org/10.1016/j.jhazmat.2016.08.067.
West, R., 1984. Solid State Chemistry and its Applications. John Wiley & Sons Ltd., New York.
Williams, L., Watson, R.E., DeSesso, J.M., 2012. Developmental and reproductive outcomes in humans and animals after glyphosate exposure: A critical analysis. J. Toxicol. Environ. Health, Part B 15, 39–96. https://doi.org/10.1080/10937404.2012.632361.
Woodbruen, A.T., 2000. Glyphosate: production, pricing and use world-wide. Pest Manag. Sci. 56, 309–312. https://doi.org/10.1002/(SICI)1526-4998(200004)56:4<309::AID-PS143>3.0.CO;2-C.
Xue, W., Zhang, G., Xu, X., Yang, X., Liu, C., Xu, Y., 2011. Preparation of titania nanotubes doped with cerium and their photocatalytic activity for glyphosate. Chem. Eng. J. 167, 397–402. https://doi.org/10.1016/j.cej.2011.01.007.
Yagub, M.T., Sen, T.K., Afroze, S., Ang, H.M., 2014. Dye and its removal from aqueous solution by adsorption: A review. Adv. Colloid Interface Sci. 209, 172–184. https://doi.org/10.1016/j.cis.2014.04.002.
Yang, Y., Deng, Q., Yan, W., Jing, C., Zhang, Y., 2018. Comparative study of glyphosate removal on goethite and magnetite: adsorption and photodegradation. Chem. Eng. J. 325, 581–589. https://doi.org/10.1016/j.cej.2018.07.058.
Yamaguchi, N.U., Bergamasco, R., Hamoudi, S., 2016. Magnetic $MnFe_2O_4$-graphene hybrid composite for efficient removal of glyphasate from water. Chem. Eng. J. 295, 391–402. https://doi.org/10.1016/j.cej.2016.03.051.
Zhang, C., Hu, X., Luo, J., Wu, Z., Wang, L., Li, B., Wang, Y., Sun, G., 2015. Degradation dynamics of glyphosate in different types of citrus orchard soils in China. Molecules 20, 1161–1175. https://doi.org/10.3390/molecules20011161.
Zhou, C., Jia, D., Liu, M., Liu, X., Li, C., 2017. Removal of glyphosate from aqueous solution using nanosized copper hydroxide modified resin: equilibrium isotherms and kinetics. J. Chem. Eng. Data 62, 3585–3592. https://doi.org/10.1021/acs.jced.7b00569.